For the sake of completeness, a computation was also carried out for values of parameters corresponding to a class (II) solid, i.e., for a solid in which the low-level hole lifetime is appreciably longer than the corresponding electron value, in the absence of trapping. The resulting characteristic, for which $\eta=1$, $V=10^{-3}$, is shown in Fig. 5. Although the values of $\mho$ involved are rather smaller than those involved in the previous results, the form of the characteristics is extremely similar, as one expects from consideration of the symmetry present in the problem.

Note added in proof. K. L. Ashley and A. G. Milnes have recently reported [J. Appl. Phys. **37**, 369 (1964)] an analysis of the region of the characteristic below, and up to, the threshold. This also demonstrates that the "threshold voltage" is different if the centers are not completely filled at thermal equilibrium.

ACKNOWLEDGMENTS

The author is indebted to A. H. Erlund, who supervised the computation, to Dr. J. Franks and Dr. P. D. Fochs for their advice and encouragement and to Dr. M. E. Haine for permission to publish this article.

PHYSICAL REVIEW VOLUME 135, NUMBER 5A 31 AUGUST 1964

Anelastic and Dielectric Relaxation due to Impurity-Vacancy Complexes in NaCl Crystals*

R. W. Dreyfus and R. B. Laibowitz†
IBM Watson Research Center, Yorktown Heights, New York
(Received 8 April 1964)

Appreciable pairing of divalent metallic impurities with Na^+ vacancies occurs in NaCl below 300°C. The reorientation of such pairs or complexes had previously been observed under an applied electric field. In the present work stress-induced reorientation of pairs in NaCl doped with $CaCl_2$ and $MnCl_2$ has been studied by means of internal friction measurements. An internal friction peak attributed to pair reorientation under stress was observed near 100°C for a vibration frequency of ~10 kc/sec. Data obtained for longitudinal stress along both the ⟨100⟩ and ⟨111⟩ crystal directions yields information about the rates of relaxation corresponding to various mechanical relaxational modes. The data can be interpreted consistently in terms of an extension of the theory previously applied to dielectric relaxation, according to which the paired vacancy occupies only nearest-neighbor (n.n.) and next-nearest-neighbor (n.n.n.) sites to the impurity. Relations obtained between the relaxation rates and the various possible jump rates for a Na^+ ion into the vacancy enable each of the specific vacancy jump rates to be determined. It is concluded that the most rapid means for the reorientation of an impurity-vacancy pair between two n.n. sites is for the vacancy to move via a n.n.n. site. The rate of jump of the impurity ion into the vacancy is found to be a relatively slow process.

I. INTRODUCTION

THE addition of divalent metallic ions to alkali halide crystals introduces an equal number of positive ion vacancies, in order to maintain charge neutrality.[1] Below a temperature of ~300°C, each of these vacancies is bound to a divalent impurity ion by electrostatic attraction. This impurity-vacancy complex can be viewed as an electric dipole, since the impurity ion has an excess positive charge while the vacancy is the center of an excess negative charge. Such a dipole can reorient by means of suitable vacancy jumps. Several workers[1–3] have observed dielectric relaxation in doped alkali halide crystals due to the reorientation of these dipoles in the presence of an electric field. Most experiments measure the dielectric loss arising from the fact that a component of the polarization is 90° out of phase with an ac electric field.[1,2] If this process is a simple one, involving only a single relaxation time, this loss as a function of frequency ω takes the form of the well-known Debye peak:

$$\tan\delta=\Delta(\omega/\zeta+\zeta/\omega)^{-1}, \quad (1)$$

where δ is the "loss angle" by which the polarization lags behind an alternating field. Here the constant Δ is the relaxation strength, while ζ is the relaxation rate (or reciprocal relaxation time). The second type of experiment observes the relaxation as an exponentially decaying polarization current j following the application of a dc field E. For the case involving a single relaxation time this takes the form[3,4]

$$j=\Delta(\epsilon E\zeta/4\pi)\exp(-\zeta t), \quad (2)$$

* Work supported in part by the U. S. Atomic Energy Commission.

† Present address: Cornell University, Department of Engineering Physics.

[1] A. B. Lidiard, in *Handbuch der Physik*, edited by S. Flügge (Springer-Verlag, Berlin, 1957), Vol. 20, p. 246.

[2] Y. Haven, J. Chem. Phys. **21**, 171 (1953); S. Jacobs, Naturwiss. **42**, 575 (1955).

[3] R. W. Dreyfus, Phys. Rev. **121**, 1675 (1961).

[4] E. R. von Schweidler, Ann. Physik **24**, 711 (1907).

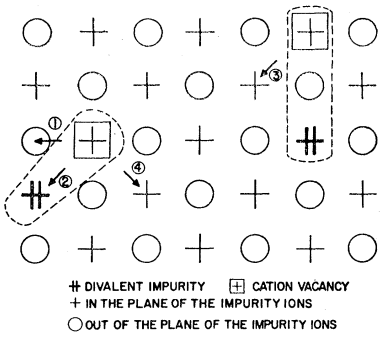

FIG. 1. Cation lattice showing n.n. and n.n.n. vacancy-impurity pairs, and the four vacancy jumps. Circles represent positive ions above and below the plane of the page by $\frac{1}{2}$ the lattice parameter. The rates corresponding to the vacancy jumps 1, 2, 3, and 4 are w_1, w_2, w_3, and w_4, respectively.

where ζ and Δ are the same quantities which appear in Eq. (1), ϵ is the dielectric constant, and t is the time after application of the electric field. For a more general relaxation spectrum, Eq. (1) becomes a sum of Debye peaks, while Eq. (2) is a sum of exponentials.

In order to interpret dielectric relaxation experiments on doped crystals in a realistic way, Lidiard[5] suggested a model which allows the vacancy to be a nearest neighbor (n.n.) or a next-nearest neighbor (n.n.n.) to the impurity ion, but which prohibits further dissociation.[6] The differential equations, set up by Lidiard, describe the rates of change of the numbers of dipoles of different orientations in terms of four vacancy jump rates: w_1, w_2, w_3, w_4. These four rates are the probabilities/sec for the four possible types of vacancy motion which are shown in Fig. 1. Thus, for example, w_4 is the probability/sec that a specific n.n.n. alkali ion jumps into a specific n.n. vacancy.[7] The solution to Lidiard's equations was shown[3] to correspond to two relaxational modes (in the ac experiment to the sum of two Debye peaks, and in the dc case to the sum of two exponentials). The two rates of relaxation, ${}_1\zeta_E$ and ${}_2\zeta_E$, which describe the time dependence of the relaxation process in an electric field are given by

$$ {}_1\zeta_E = w_1+w_2+2w_3+w_4 + [(w_1+w_2-2w_3+w_4)^2+4w_3w_4]^{1/2}, \quad (3) $$

$$ {}_2\zeta_E = w_1+w_2+2w_3+w_4 - [(w_1+w_2-2w_3+w_4)^2+4w_3w_4]^{1/2}. \quad (4) $$

An expression can also be obtained for each of the magnitudes of the corresponding relaxation strengths, Δ_1 and Δ_2. Experimentally, only the ratio Δ_1/Δ_2 is useful, because an independent reliable estimate of the total concentration of complexes in the form of simple dipoles is not readily available. Since the dielectric experiments provide at most three measureable quantities (i.e., ${}_1\zeta_E$, ${}_2\zeta_E$, and Δ_1/Δ_2), it was not possible in the earlier work[3] to determine all the four vacancy jump rates (w's) independently. Furthermore, for most of the divalent impurities studied, the magnitude of the faster of the two relaxations was quite small, so that precise values of ${}_1\zeta_E$ and of Δ_1/Δ_2 were not available either. Thus, only the quantity ${}_2\zeta_E$ is measured with some precision. In order to obtain further information, the size of the impurity ion was varied (in NaCl) over the range from 0.7 to 1.2 times the Na^+ radius.[3] The following conclusions were obtained: (1) In the case of large impurity ions, the major relaxation involves the reorientation of n.n. dipoles by vacancy jumps from one n.n. site to another n.n. site (rate w_1). (2) For impurity ions smaller than Na^+, the relaxation rate is accelerated due to the increased value of w_2, the rate of jump of the impurity ion into the vacancy. (3) As the radius of the impurity ion decreases, the fraction of vacancies occupying n.n.n. sites increases.

In the present paper, a second method is used to study the possible jumps of the impurity-vacancy pair in alkali halides. This method consists of observing the *anelastic relaxation*, which takes place when the crystal is subjected to an applied stress field. The fact that the symmetry about the defect is lower than cubic means that this defect is an "elastic dipole" and therefore capable of reorientation under an applied stress.[8] In this sense it is analogous to the impurity-impurity pair, which is responsible for the well-known "Zener relaxation" in alloys.[9] Under alternating stress, the strain produced by the reorientation of defects lags behind the stress and therefore gives rise to an anelastic loss or internal friction. If δ is the phase lag of the total strain behind the stress, the Debye type equation (1), or more generally, a sum of such Debye expressions, may be expected to apply here in the same way as it did in the case of dielectric loss.

It is well known that stress will excite different "relaxational modes" (i.e. it will produce a different repopulation of sites) than will an electric field.[10] Accordingly, one may anticipate that the relaxation rates (ζ's) obtained from anelastic experiments will involve the jump rates (w's) in different combinations than in Eqs. (3) and (4), thereby giving further independent relations in the four jump rates. An additional advantage of stress experiments is that there are three independent elastic compliances in a cubic crystal, each one of which may show relaxation behavior with a different relaxation rate. This contrasts with the fact that a cubic crystal has only one dielectric constant. The relationships between anelastic relaxation rates and

[5] A. B. Lidiard, *Bristol Conference Report on Defects in Crystalline Solids, 1954* (The Physical Society, London, 1955), p. 283.

[6] Since the position of the chlorine ions does not enter directly into the present discussion, the terminology "n.n." and "n.n.n." will refer only to sodium-ion positions.

[7] In the recent literature, some authors have interchanged these definitions of w_3 and w_4.

[8] A. S. Nowick and W. R. Heller, Advan. Phys. **12**, 251 (1963).

[9] See, for example, A. S. Nowick and D. P. Seraphim, Acta Met. **9**, 40 (1961).

[10] J. B. Wachtman, Jr., Phys. Rev. **131**, 517 (1963).

vacancy jump rates are derived in the next section. (This problem has also been treated by group-theoretical methods, first by Haven and van Santen,[11] and most recently by Franklin.[12]) The rest of this paper is then devoted to obtaining values for the various jump rates from experimentally measured relaxation rates.

A similar study of defect relaxation under both stress and electric field was carried out by Wachtman[10] for the case of a paired defect in doped ThO_2. Since only a single mode (i.e., a simple Debye peak) appeared both in the dielectric and anelastic cases, it was only necessary for him to consider nearest-neighbor configurations to account for the behavior.

II. THEORY

Since the internal friction experiments are most conveniently carried out in longitudinal or flexural vibration, the appropriate elastic modulus which changes as a result of the defect relaxation is Young's modulus E along the length of the sample. The total relaxation strength Δ is defined[13] as $\Delta=\delta E^{-1}/E^{-1}$, where δE^{-1} is the change in compliance (reciprocal Young's modulus) due to the defect reorientations. The value of E^{-1} depends, for a cubic crystal, on the three elastic compliances s_{11}, s_{12}, and s_{44}. These compliances are conveniently recombined[13] to form the constants $s\equiv s_{44}$, $s'\equiv 2(s_{11}-s_{12})$, and $s''\equiv s_{11}+2s_{12}$. The advantage of using the latter quantities is that s and s' are two simple shear constants while s'' is $\frac{1}{3}$ the hydrostatic compressibility.[14] Furthermore, if the longitudinal stress axis of the crystal used is ⟨100⟩ or ⟨111⟩, the relaxation δE^{-1} involves only *one* of the two shear relaxations δs and $\delta s'$.[13] Thus,

$$\delta E_{\langle 100\rangle}^{-1}=\tfrac{1}{3}(\delta s'+\delta s''), \tag{5}$$

$$\delta E_{\langle 111\rangle}^{-1}=\tfrac{1}{3}(\delta s+\delta s''). \tag{6}$$

Equation (5) implies that flexural or longitudinal vibration of a crystal rod whose axis is along ⟨100⟩ excites those changes in defect orientations (relaxational normal modes) which distort the crystal as does an s'-type shear combined with a bulk relaxation; similarly for a ⟨111⟩ crystal and the s-type shear. The hydrostatic relaxation $\delta s''$ can occur in both cases through an interchange of populations between the two defect types (i.e., n.n. and n.n.n.).[8]

TABLE I. Equivalent and nonequivalent vacancy sites under an applied longitudinal stress.

Stress direction	Type of site	Location of sites [impurity at (0,0,0)]	Number of sites
⟨100⟩	a	$(0, \pm\frac{1}{2}, \pm\frac{1}{2})$	4
	b	$(\pm\frac{1}{2}, \pm\frac{1}{2}, 0)$; $(\pm\frac{1}{2}, 0, \pm\frac{1}{2})$	8
	c	$(0, \pm1, 0)$; $(0, 0, \pm1)$	4
	d	$(\pm1, 0, 0)$	2
⟨111⟩	e	$\pm(\frac{1}{2}, \frac{1}{2}, 0)$; $\pm(\frac{1}{2}, 0, \frac{1}{2})$; $\pm(0, \frac{1}{2}, \frac{1}{2})$	6
	f	$\pm(\frac{1}{2}, -\frac{1}{2}, 0)$; $\pm(0, \frac{1}{2}, -\frac{1}{2})$; $\pm(\frac{1}{2}, 0, -\frac{1}{2})$	6
	g	$(\pm1, 0, 0)$; $(0, \pm1, 0)$; $(0, 0, \pm1)$	6

The method which will be used to obtain the anelastic relaxation rates is essentially the same as that applied previously to the dielectric relaxation problem.[3,5] The effect of the stress is to perturb the jump rates of vacancies among the various available sites. First, we calculate the time dependence of the number of pairs in each orientation when a small constant stress is applied at time $t=0$. The time dependence of the approach to equilibrium will be a sum of exponentials each of the form $1-\exp(-\zeta t)$. Under an alternating stress field, each exponential transforms to a Debye peak governed by the same relaxation rate ζ.

For the determination of the relaxation rates under a ⟨100⟩ oriented longitudinal stress, we begin by listing the groups of n.n. and n.n.n. sites which are equivalent under the applied stress, as given in Table I. The total concentration of vacancies at sites of type $a, \cdots, d$, are designated by $n_a, \cdots, n_d$, respectively. The rates of change of the concentrations at each type of site are related to the various jump rates by the following equations:

$$\dot{n}_a=-4n_aw_1(1+R)-2n_aw_4(1-S)+4n_bw_1(1-R)+2n_cw_3(1+S), \tag{7}$$

$$\dot{n}_c=2n_aw_4(1-S)+2n_bw_4(1-R-S)-2n_cw_3(1+S)-2n_cw_3(1+R+S), \tag{8}$$

$$\dot{n}_d=4n_bw_4(1+T)-4n_dw_3(1-T), \tag{9}$$

where R is the fractional increase in the rate of a jump from an a to a b type site caused by the stress; similarly, S is the fractional increase for the c to a jump, and T for b to d. The corresponding rates in the absence of stress are w_1, w_3, and w_4, respectively. For the anelastic (low stress) range, R, S, and T are small ($\ll1$) and proportional to the applied stress. A fourth differential equation (in $\dot{n}_b$) is not an independent equation, because the total number of vacancies in both n.n. and n.n.n. sites is conserved:

$$N_i=4n_a+8n_b+4n_c+2n_d. \tag{10}$$

The above equations yield a set of three linear homogeneous differential equations. Possible solutions are

[11] Y. Haven and J. H. van Santen, Nuovo Cimento **7**, 605 (1958).

[12] A. D. Franklin, J. Res. Natl. Bur. Std. **67A**, 291 (1963). There are some misprints in the designations of the irreducible representations in this paper.

[13] C. Zener, *Elasticity and Anelasticity of Metals* (University of Chicago Press, Chicago, 1948).

[14] The constant s is the shear compliance for a shearing stress applied across an (100) plane in the [010] direction, s' is the shear compliance for a (110) [1$\bar{1}$0] shear, and s'' is $\frac{1}{3}$ the hydrostatic compressibility. For convenience, in this paper we designate the first type of shear strain as the "s-type" and the second as the "s'-type" shear. For comparison with the group theoretical approach, it should be noted that the s- and s'-type shears transform, respectively, as the irreducible representations T_{2g} and E_g, while hydrostatic strain transforms as the representation A_{1g} of the full cubic point group.

exponentials of the form

$$n_i = n_i^{(0)}[1+\alpha_i(1-e^{-\zeta t})], \tag{11}$$

where the index i represents a, b, c, or d, α_i is the fractional change in n_i when equilibrium ($t\to\infty$) is reached, and ζ is a permissible relaxation rate (i.e., eigenvalue). In substituting Eq. (11) into Eqs. (7)–(10) terms in $\exp(-\zeta t)$ may be separately equated, dropping second-order terms of the type $\alpha_a R$. This results in a set of three homogeneous linear algebraic equations. The condition for a nontrivial solution is, as usual, that the determinant of the coefficients must vanish. This gives the following three eigenvalues for ζ:

$$_1\zeta_{s'} = 3w_1+2w_3+w_4 + [(3w_1-2w_3+w_4)^2+2w_3w_4]^{1/2}, \tag{12}$$

$$_2\zeta_{s'} = 3w_1+2w_3+w_4 - [(3w_1-2w_3+w_4)^2+2w_3w_4]^{1/2}, \tag{13}$$

$$\zeta_{s''} = 4w_3+2w_4. \tag{14}$$

The subscripts s' and s'' are added to the relaxation rates in order to distinguish the hydrostatic from the shear modes of relaxation. The presence of both types of relaxation is shown by Eq. (5). The identification of the hydrostatic relaxation rate $\zeta_{s''}$ is based upon the fact that the rate $4w_3+2w_4$ also occurs for a crystal oriented in the ⟨111⟩ direction, as will be shown below. (Also, it can easily be obtained directly by considering separately the case of a hydrostatic stress applied to the crystal.) The two relaxation rates $_1\zeta_{s'}$ and $_2\zeta_{s'}$ may be interpreted as essentially n.n. or n.n.n. type relaxations in the manner shown in Ref. 3, Eqs. (14)–(21).

The corresponding equilibrium occupations, $n_i^{(0)}\alpha_i$, which are essentially the relaxational normal modes, are also readily obtained.

The derivation of the relaxation time constants which are excited by stress along a ⟨111⟩ oriented crystal is carried out in the same manner as for the ⟨100⟩ case. The three types of vacancy sites e, f, g are defined in Table I. The equations which govern the time dependent concentration at each type of site are as follows:

$$\dot{n}_e = -2w_1n_e(1+U)-2w_4n_e(1-V) +2w_1n_f(1-U)+2w_3n_g(1+V), \tag{15}$$

$$\dot{n}_g = 2w_4n_e(1-V)+2w_4n_f(1-W) -2w_3n_g(1+V)-2w_3n_g(1+W), \tag{16}$$

with

$$N_i = 6n_e+6n_f+6n_g, \tag{17}$$

where the appropriate fractional rates of change for the vacancy jump rates are given by U, V, and W. Solutions for the relaxation rate are found by the same procedure as in the previous case. Only two relaxation rates now appear, as follows:

$$\zeta_s = 4w_1+2w_4, \tag{18}$$

$$\zeta_{s''} = 4w_3+2w_4. \tag{19}$$

The presence of only one relaxation rate associated with a shear mode is related to the fact that a ⟨111⟩ stress axis produces no preference (and therefore no reorientation) among the various equivalent n.n.n. sites. The s-type mode which is excited is specifically related to the reorientation of n.n. complexes under this stress.

It is interesting to note that w_2, the rate associated with the jump which produces a 180° reversal of the n.n. pair, does not enter into any of the anelastic relaxation rates. This is due to the fact that stress is centrosymmetric and therefore cannot produce a preference between two orientations which differ by 180°.

In summary, anelastic measurements, using both ⟨100⟩ and ⟨111⟩ oriented crystals offer the opportunity to measure four relaxation rates ζ_s, $_1\zeta_{s'}$, $_2\zeta_{s'}$, $\zeta_{s''}$, each of which is expressible in terms of the three jump rates w_1, w_3 and w_4. In view of the fact that each of the ion jump rates $w_j (j=1,\cdots,4)$ varies according to an Arrhenius relation of the form

$$w_j = w_{j0}\exp(-\epsilon_j/kT), \tag{20}$$

it is anticipated that each relaxation rate ζ will in turn obey a similar equation with an appropriate activation energy given by that of the dominant w_j.

III. EXPERIMENTAL METHOD

Doped samples were prepared either by diffusing[3] various metallic chlorides into commercial (Harshaw or Optovac) NaCl or by the Kyropolous technique.[15] In all cases the impurity level was checked by spectroscopic analysis. The ⟨100⟩ oriented samples were cleaved while the ⟨111⟩ samples were cut from a bulk single crystal by a wet string saw and lapped on wet silk to final shape.

In the internal friction experiment, rectangular bars of NaCl are driven at their fundamental frequency of vibration. After mechanical energy has been imparted

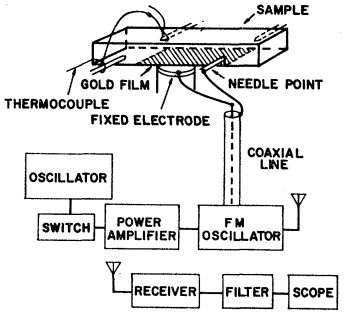

FIG. 2. Schematic illustration of the experimental arrangement for excitation and observation of the decay of flexural vibrations in NaCl bars. The electrical components are Hewlett Packard No. 650A test oscillator, General Radio No. 1206B unit amplifier, Hallicrafter S×62A receiver, Khron Hite variable band pass filter and Tektronix 545A oscilloscope.

[15] R. W. Dreyfus, in *The Art and Science of Growing Crystals*, edited by J. J. Gilman (John Wiley & Sons, Inc., New York, 1963), p. 410.

to the sample, the drive is switched off and the free-decay time of the sample vibrations is measured. The number of cycles N for the vibration amplitude to decrease by e^{-1} is obtained and the logarithmic decrement calculated from $\log \text{dec} = 1/N = 1/f\tau$ where f is the sample vibration frequency and τ is the exponential decay time of vibration. This quantity is related to the phase angle δ by which the strain lags behind the stress by[13]

$$\tan\delta = (\log \text{dec})/\pi. \quad (21)$$

In all of the present internal friction experiments, measurements are made as a function of temperature T. It is clear that a Debye peak of the type given by Eq. (1) may be traced out by varying either ω or ζ. In the present case, it is convenient to keep ω fixed at the value equal to the resonant frequency of the vibrating bar. In view of the exponential-type dependence of ζ on $1/T$, which follows from Eq. (20), a Debye peak (or group of such peaks) is most conveniently traced out by varying the temperature.

The experimental arrangement is illustrated in Fig. 2. The sample, as shown at the top of the diagram, is supported at its flexural nodes. Vibrations are induced by electrostatic attraction between a fixed electrode and a gold film evaporated onto the sample. The gold film is connected to one of the needle points by a narrow line of silver paint. The resonant frequency of the sample, which is determined by its size and the method of support, falls in the range of 3–20 kc/sec. In a few cases higher frequencies were obtained by using longitudinal vibrations and supporting the sample (vertically) at its midpoint. The frequency of the drive voltage is half the resonant frequency of the sample due to the fact that the sample is attracted by both positive and negative voltages. Drive voltages in the range 10–100 V produced strain amplitudes of 10^{-6}–10^{-5}.

The detection scheme is a frequency modulation method which utilizes the capacitance between the gold film on the sample and the fixed electrode placed in the tank circuit of a radio-frequency oscillator. The center frequency of the oscillator is approximately 85 Mc/sec. The rf signal is picked up on a suitable receiver, filtered and then displayed on an oscilloscope. A permanent

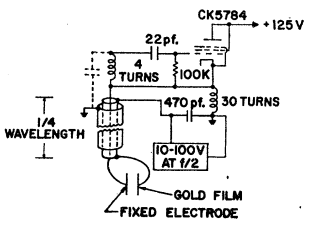

FIG. 3. The circuit of the frequency modulated oscillator which detects the vibration of the sample. The gold film to electrode capacity at the end of the coaxial line looks like an inductance to the FM oscillator. The frequency of the oscillator is determined by this inductance plus the 4-turn coil and the distributed capacitance.

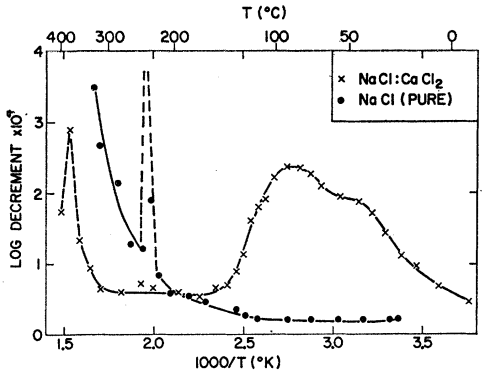

FIG. 4. Comparison of internal friction curves for pure and $CaCl_2$-doped NaCl crystals stressed in the ⟨100⟩ direction at 8.5 kc/sec, showing the broad peak for the doped crystal. (The sharp peaks near 240 and 400°C are attributed to the straining of the samples by the supporting wires.)

record of the decay is obtained in the form of a photograph of the scope face. Similar arrangements have been reported by previous authors.[16]

The circuit shown in Fig. 3 is arranged to minimize the influence of the audio drive frequencies upon the FM oscillator. This was advantageous in finding the resonant frequency of the sample, since the buildup of vibrations could be observed. Similar (but somewhat more complicated) circuits with two coaxial lines had been utilized previously.[16]

The sample was supported at the vibrational nodes by two different methods. In some of the earlier measurements, two wires were strung over pairs of ceramic supports. One of the two wires was a platinum to platinum-rhodium thermocouple with the junction under the sample, while the excitation voltage was applied through the other wire. These wires were affixed to the sample with high-temperature cement. With this method sharp peaks appeared in some of the plots of damping versus temperature. Properties of these peaks are: (1) They do not easily anneal out at temperatures up to 400°C; (2) they are generally around 2 orders of magnitude above the background; (3) the peaks erratically move from one temperature to another; and (4) the peak widths are as small as 2°C. These characteristics suggest that the peaks are spurious, i.e., not related to an intrinsic property of the sample. They were in fact attributed to the straining of the sample by the support wires and/or the adhesive. It was found that one way to eliminate the above peaks was to use needle points for sample supports as shown in Fig. 2. Satisfactory needle points were osmium-iridium-tipped phonograph needles.

After mounting, the samples were heated to about 400°C in a vacuum of less than 1 μ, where they

[16] P. G. Bordoni and M. Nuovo, Acustica **4**, 184 (1954); D. O. Thompson and F. M. Glass, Rev. Sci. Instr. **29**, 1034 (1958); P. D. Southgate, J. Sci. Instr. **36**, 284 (1959); L. J. Bruner, Phys. Rev. **118**, 399 (1960).

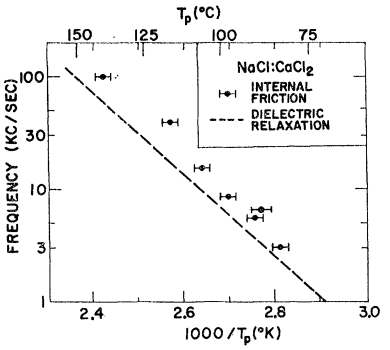

FIG. 5. Plot of vibration frequency versus reciprocal peak temperature for ⟨100⟩ oriented NaCl:$CaCl_2$. Also shown (as the dashed line) are the earlier dielectric relaxation results.

were held for about 15 h, and then cooled at a rate between 1 and 2°C/min while simultaneously measuring the damping. Data taken during the initial heat-up showed large background damping. On the other hand, the data on cooling generally showed low background damping and agreed closely with data taken on subsequent reheating.

The sample was heated by a resistance furnace wound on a copper cylinder which was mounted inside a vacuum chamber. Cooling coils were also welded to the copper cylinder to permit attainment of temperatures down to −100°C. The temperature, or the heating and cooling rate, was controlled electronically.

Dielectric relaxation measurements were also made in the present apparatus using an ac bridge. For these measurements, a thin crystal was supported in approximately the same position in the apparatus as the sample on which internal friction was measured.

IV. EXPERIMENTAL RESULTS

The initial internal friction measurements were directed toward finding anelastic damping peaks caused by the presence of impurity-vacancy complexes in ⟨100⟩ oriented samples. In this connection, information already available from dielectric loss peaks, particularly the knowledge of the temperature at which the peak occurs, was most useful. Typical results for the internal friction measurements are shown in Fig. 4. It is clear that a broad peak appears for the intentionally doped sample but not for a relatively pure sample, i.e., one containing <10-ppm $CaCl_2$. These results are similar to dielectric relaxation results, in that intentional doping enhances the magnitude of loss peaks and also in the approximate temperature range at which the peak occurs. The sharp spikes which occur above 200°C are attributed to the wire supports used in this early run, as discussed in the previous section.

The resonant frequencies of the $CaCl_2$-doped samples were varied over the range of 3–100 kc/sec, in order to obtain the activation energy associated with the relaxation peak. To find the temperature T_p of maximum damping, the background damping was interpolated and subtracted from the data. Figure 5 shows the results for the variation of $1000/T_p$ as a function of the frequency of vibration for Ca^{++}-doped samples, and compares these with previous[3] dielectric relaxation rates. It is noteworthy that the mechanical relaxation rates are higher than the dielectric. Nevertheless, within experimental error, essentially the same activation energy (~0.7 eV) is involved in both cases. Similar results were obtained for $MnCl_2$-doped crystals.

The internal friction peaks are given in Fig. 6 for NaCl crystals which contain various impurities. In addition, comparison with Fig. 4 shows that the peak for the $CaCl_2$-doped sample differs from all of these. It may therefore be concluded that the shape and position of the peak depends on the particular impurity. Previous measurements of dielectric relaxation[3] had shown that the dielectric peaks depended on the identity of the impurity in the same way. An internal friction peak due to impurity-vacancy complexes was also looked for in the system NaCl:$ZnCl_2$ (300 ppm), but no peak was detected in five runs, even though the background was low.

It should be noticed that the ordinate in Fig. 6 and subsequent figures is the product $T\times$log dec. This choice is based on the fact that for small defect concentrations the relaxation strength Δ [Eq. (1)] is proportional[8] to $1/T$. For a simple Debye peak, the plot of $T\times$log dec versus $1/T$ therefore results in a symmetrical peak, provided that ζ obeys a simple Arrhenius equation.

It should be recalled that all internal friction data reported thus far are for ⟨100⟩ oriented crystals. In Sec. II it was shown that the flexural vibration of such crystals involves only the s'-type shear modes. In order to obtain information on the other (s-type) shear mode, a $CaCl_2$-doped crystal was cut with a ⟨111⟩ crystallographic axis oriented lengthwise. Figure 7 compares the anelastic damping in such a crystal to the data for a ⟨100⟩ crystal from the same ingot. The most apparent change in the data for the ⟨111⟩ orientation is that the peak has been considerably narrowed compared to the ⟨100⟩ peak. The ⟨111⟩ peak is also found to be five times

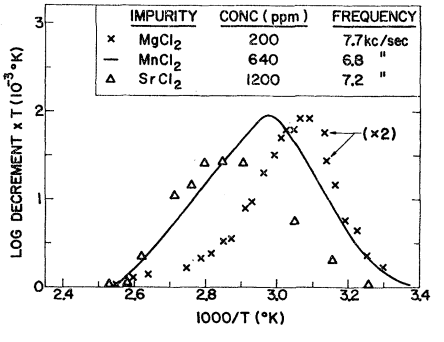

FIG. 6. Comparison of the internal friction peaks for NaCl crystals doped with various divalent cations.

smaller than the ⟨100⟩ peak. It is difficult to use the peak heights for quantitative purposes, however, since the heat treatments of the two samples were never identical.

In a similar way Fig. 8 contrasts the data for a $MnCl_2$-doped crystal in the ⟨100⟩ and ⟨111⟩ orientations. The ⟨100⟩ peak for the $MnCl_2$-doped sample is broadened on the higher temperature side, in contrast to the results for the Ca^{++}-doped sample. The internal friction measurements for the ⟨111⟩ oriented crystal show that the peak is again more sharply defined for this orientation. A comparison of the peak in Fig. 8 with the corresponding peak in Fig. 6 offers the opportunity to note any differences due to varying concentration of $MnCl_2$, since the two samples contained 15 and 640 ppm of impurity, respectively. It is observed, however, that although the peak heights are different, there is no significant concentration dependence of the peak shape and position.

In summary, the collection of facts presented leads to the conclusion that the internal friction peaks are due to impurity-vacancy complexes. These facts are (a) that no peak occurs in the absence of divalent impurities, (b) the approximate agreement between the location of the anelastic and dielectric loss peaks, (c) the essential agreement between the activation energy for anelastic and dielectric relaxation, and (d) the dependence of peak position and shape on the specific divalent impurity ion. With respect to the last point, no such dependence would be expected if the peak were in any way due to free vacancies introduced by the impurity ions. In addition, the data which compares the internal friction of ⟨100⟩ and ⟨111⟩ oriented crystals will be useful toward the quantitative analysis of the anelastic relaxation rates in terms of specific ion jump rates. This analysis will be carried out in the next section.

V. DEDUCTION OF JUMP FREQUENCIES

The first step in the analysis of the data is to consider the shape of the internal friction peaks. In the Theory

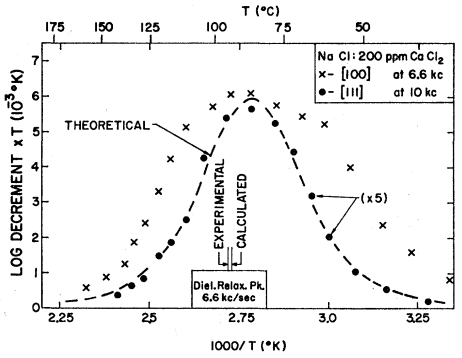

FIG. 7. A comparison of internal friction peaks for NaCl:$CaCl_2$ crystals oriented in the ⟨100⟩ and ⟨111⟩ directions. The curve marked "theoretical" is a single Debye peak for an activation energy of 0.7 eV. In addition, the calculated and measured positions of the dielectric relaxation peak are noted.

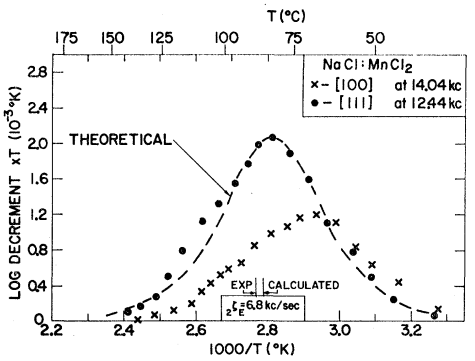

FIG. 8. Same type of comparison as in Fig. 7 for two NaCl: (15 ppm) $MnCl_2$ samples from the same ingot.

section it was indicated that a single mode of relaxation should produce a simple Debye peak. Such a peak should be symmetrical in the plot of $T\tan\delta$ (or $T\times$log dec) versus $1/T$. In contrast, the peaks for the ⟨100⟩ oriented crystals are generally not symmetrical. Furthermore, they are too wide to be represented by a simple Debye peak. This may be seen from the fact that the width at half-maximum of a Debye peak, in a plot versus $1/T$, is given [from Eq. (1) combined with an Arrhenius equation for ζ] by

$$\delta(1000/T)=0.227/\epsilon, \qquad (22)$$

where ϵ is the activation energy in eV. With the aid of this equation it is possible to analyze a broad internal friction peak into a small number of Debye peaks. In the present study it was found that a change in frequency causes a shift of the peak with no detectable change in shape (for shifts up to 60°C). This result implies that the activation energies of the component Debye peaks are not much different from each other, and from the average value of very nearly 0.7 eV. Accordingly, the data have been analyzed into component Debye peaks with widths given by Eq. (22), taking $\epsilon=0.70$ eV for all component peaks. (It was checked, however, that small modifications of the activation energies of the component peaks do not appreciably alter the results of the analysis.) Using this method, it was found that three Debye peaks are necessary to fit satisfactorily the experimental results for the ⟨100⟩ oriented crystals. An example is given in Fig. 9, where the experimental points can be fitted by Debye peaks located at 57, 81, and 109°C. The significance of these peak temperatures is that they represent, in each case, the temperature at which the relaxation rate ζ is equal to ω, the angular frequency at which the experiment was carried out. In a similar way, the ⟨100⟩ peak for the $MnCl_2$-doped crystal was analyzed into subpeaks.

In contrast, the peak for the ⟨111⟩ oriented $CaCl_2$-doped crystal can be fitted by a single Debye peak corresponding to $\epsilon=0.70$ eV (see Fig. 7). For the $MnCl_2$-

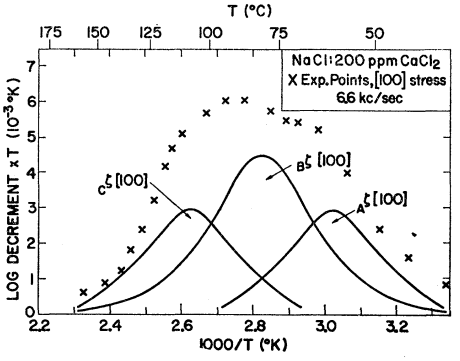

FIG. 9. The decomposition of the experimental results from Fig. 7 into three Debye peaks, based upon the assumption that the component peaks have half-widths given by an activation energy of 0.7 eV.

doped crystal the same is true except for a small subpeak located on the high temperature side, as shown in Fig. 8.

For comparison purposes it is desirable to express the appropriate relaxation rates all at the same selected temperature. For this purpose the Arrhenius equation gives

$$\zeta(T_1)/\zeta(T_2)=\exp[(\epsilon/k)(T_2^{-1}-T_1^{-1})]. \quad (23)$$

This equation permits the conversion of a ζ value from temperature T_2 to temperature T_1. In the present case, the reference temperature selected was 87°C, since this is the temperature at which the ⟨111⟩ peak occurred for the $CaCl_2$-doped crystal. Using Eq. (23) with $\epsilon=0.70$ eV enabled the other ζ values to be corrected to 87°C. These values of the relaxation rates for both the $CaCl_2$- and $MnCl_2$-doped samples are listed in Table II. The notation used identifies the relaxation rate of the component peaks with prefix A, B, and C in the order of decreasing value for both the ⟨100⟩ and ⟨111⟩ orientations. These specific values for the relaxation rates were established by making a least-squares fit to all the data. In the case of the ⟨100⟩ peak in NaCl:$MnCl_2$, the small size of the subpeaks produces greater uncertainty in the analysis than for the NaCl:$CaCl_2$.

Another way of showing that the decomposition of the ⟨100⟩ peaks is consistent for the various NaCl:$CaCl_2$ samples measured at different frequencies is to plot the relaxation rate ($=2\pi f$) versus reciprocal peak temperature, as in Fig. 10. As can be seen from this figure,

TABLE II. Relaxation rates converted to 87°C (units of 10^4 sec^{-1}).

	NaCl:$CaCl_2$	NaCl:$MnCl_2$
${}_A\zeta\langle100\rangle$	47 ±5	34 ±5
${}_B\zeta\langle100\rangle$	5.2±0.4	8.7±1.0
${}_C\zeta\langle100\rangle$	1.0±0.3	2.3±0.7
${}_A\zeta\langle111\rangle$	6.3±0.2	10.6±0.5
${}_B\zeta\langle111\rangle$	···	2.1±0.7

the relaxation rates make up three separate groups, each of which displays an activation energy close to 0.7 eV.

Having tabulated the relaxation rates of the experimentally observed Debye peaks in Table II, it is now desirable to attempt to relate these quantities to the relaxation rates of the normal modes, derived in Sec. II. In this way we can accomplish the final objective of calculating the individual jump frequencies. Since the data from the NaCl:$CaCl_2$ samples are the more precise, it is reasonable to make use of this data in the identification of the relaxation modes. The starting point in this analysis is the identification of the relaxation rate ${}_A\zeta\langle111\rangle$. From the theoretical analysis of the ⟨111⟩ case, this rate should correspond either to the hydrostatic mode (rate $\zeta_{s''}$) or to the s-type shear mode (rate ζ_s). For a first choice we consider the ${}_A\zeta\langle111\rangle$ relaxation as the hydrostatic rate. Starting with this identification, we are led to the following tentative identifications:

$$\zeta_{s''}={}_A\zeta\langle111\rangle={}_B\zeta\langle100\rangle,$$
$$\zeta_s \text{ not identified},$$
$${}_1\zeta_{s'}={}_A\zeta\langle100\rangle,$$
$${}_2\zeta_{s'}={}_C\zeta\langle100\rangle.$$

Making use of the theoretical expressions for $\zeta_{s''}$, ${}_1\zeta_{s'}$, and ${}_2\zeta_{s'}$, we now have three relations in terms of three jump rates, w_1, w_3, and w_4. It is therefore possible to solve for the w's. Two sets of solutions exist because the theoretical relations are quadratic. One of these is physically unacceptable because it yields a large negative value for w_4. The other solution gives $w_1=69$, $w_3=2.5$, and $w_4=27$, in units of 1000 jumps/sec. Since w_3/w_4 is the ratio of populations in n.n. and n.n.n. sites, it is clear that this solution implies that at 87°C, n.n.n. dipoles exceed n.n. dipoles by 1 order of magnitude. This result is inconsistent with theoretical estimates of the relative binding energies of the two sites[17] as well as

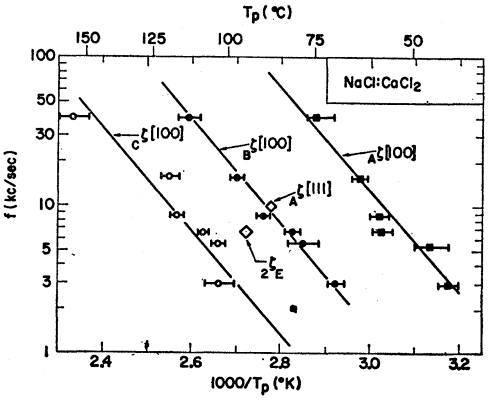

FIG. 10. The frequency of the various Debye peaks in NaCl:$CaCl_2$ as a function of reciprocal peak temperature. The lines drawn correspond to an activation energy of 0.7 eV.

[17] F. Bassani and F. G. Fumi, Nuovo Cimento **11**, 274 (1954); M. P. Tosi and G. Airoldi, *ibid.* 8, 584 (1958).

with experiments on $MnCl_2$-doped samples.[18] In addition, it is not possible to reconcile the location of the dielectric peak (i.e., the value ${}_2\zeta_E$) with this solution, since this peak would be expected to occur at a temperature at least 30° above where it is actually found. For these reasons the above identification is rejected.

The second choice is to identify ${}_A\zeta\langle 111\rangle$ as ζ_s. Several choices exist for the correlation of the theoretical relaxation rates ${}_1\zeta_{s'}$ and ${}_2\zeta_{s'}$ with the experimental rates. Only one set of correlations, however, provides a consistent set of solutions for the w's. This particular correlation of experimental and theoretical relaxation rates is as follows:

$$\zeta_s = {}_A\zeta\langle 111\rangle,$$
$$\zeta_{s''} \text{ not identified},$$
$${}_1\zeta_{s'} = {}_A\zeta\langle 100\rangle,$$
$${}_2\zeta_{s'} = {}_B\zeta\langle 100\rangle.$$

In testing this identification the w's have been calculated and are listed in Table III, column 3, along with estimates of their uncertainties. Column 4 lists the values of the w's obtained from the data on NaCl: $MnCl_2$, with the same identification as in the case of Ca^{++}. Both sets of values for the vacancy jump rates are apparently reasonable, as will be discussed in the following section.

The dielectric relaxation rate ${}_2\zeta_E$ involves not only w_1, w_3, and w_4, but also the rate w_2 of impurity-vacancy interchange. It would appear, therefore, that a knowledge of ${}_2\zeta_E$ provides a fourth equation with the opportunity to determine w_2. This belief is based on the assumption that w_2 is comparable in value to the remaining jump rates. If, of course, w_2 is much lower than the other jump rates, Eq. (4) serves only to provide a check on the values of w_1, w_3, and w_4 already obtained from the anelastic measurements. Examination of the dielectric data shows that the latter situation is indeed the case. For the $CaCl_2$-doped samples, a dielectric peak was found (at 6.6 kc/sec) to be located at 95°C. This corresponds to a rate ${}_2\zeta_E$ of 2.51×10^4 sec^{-1} at 87°C. From the data of Table III substituted into Eq. (4), assuming $w_2=0$, the value ${}_2\zeta_E=2.9\times10^4$ sec^{-1} is obtained. The peak temperature for 6.6 kc/sec is then calculated to be at 93°C. The experimental and calculated peak positions, as shown in Fig. 7, are within experimental error. Similar results for the $MnCl_2$-doped crystal are marked on Fig. 8. It is concluded that the dielectric data are consistent with the analysis of the anelastic data only if w_2 is negligible compared to w_3 and w_4.

The relaxations ${}_C\zeta\langle 100\rangle$ observed for both Ca^{++} and Mn^{++} doping, and ${}_B\zeta\langle 111\rangle$ for the Mn^{++} case only, remain to be identified. Consideration is next given to the question of whether either of these can be related to the hydrostatic relaxation $\zeta_{s''}$. Using the values of the jump rates in Table III, one can estimate the temperature at which a hydrostatic peak should appear. This turns out to be between 60 and 70°C in both Figs. 7 and 8. The unidentified peaks are at much higher temperatures, and therefore could not be associated with the hydrostatic relaxation. The absence of an observable hydrostatic relaxation in the present case is not unique. For example, for the Zener relaxation in the fcc Ag-Zn alloy the hydrostatic relaxation was also found to be too small to be detectable.[19] This must stem from the fact that the "size factor" is not much different for the n.n. and n.n.n. pairs.[8]

TABLE III. Jump rates and activation energies for vacancies associated with Ca^{++} or Mn^{++} ions.

Vacancy motion		Vacancy jump rates at 87°C (units of 10^3 sec^{-1})		Activation energy for motion (eV)	
Rate	Sites	Ca^{++}	Mn^{++}	Ca^{++}	Mn^{++}
w_3	n.n.n. → n.n.	114±10	79±14	0.63	0.65
w_4	n.n. → n.n.n.	27±6	41±15	0.68	0.67
w_1	n.n. → n.n.	2.2±1.8	5.8±7.2	0.76	>0.71

Since the above considerations eliminate the possibility of interpreting the high-temperature component peaks ${}_C\zeta\langle 100\rangle$ and ${}_B\zeta\langle 111\rangle$ in the framework of the present theory, other explanations must be considered for these peaks. At the present time, either of two explanations seems possible. Firstly, the high-temperature peaks may involve impurity-vacancy pairs which are more distant than the n.n.n. sites. Secondly, the peaks may be due to an impurity-vacancy complex located next to another impurity. The impurity might be a second complex of the same type, or an anion impurity. Such an aggregation constitutes a new type of center which correspondingly should have a different relaxation rate than the simpler defect. The present results are not adequate to distinguish between these explanations.

The value of each jump rate can be expressed in terms of an activation energy by means of Eq. (20). To obtain this activation energy requires a suitable value for the frequency factor w_{j0}. In the absence of further information, $w_{j0}=9\times10^{13}$ (sec^{-1}) is used for all the jump rates. (This value was derived from the dielectric relaxation results[3] under the approximation that ${}_2\zeta_E\approx 2w_1+w_4 \approx w_4$, which is justified on the basis of the present results that $w_3\gg w_4\gg w_1$.) Support for the assumption that w_{j0} is nearly the same for all jumps comes from the fact that the value of w_{j0} for a free vacancy is approximately the above value.[20] The activation energies deduced in this way are then listed in columns 5 and 6 of Table III.

[18] G. D. Watkins, Phys. Rev. **113**, 79, 91 (1959).

[19] D. P. Seraphim and A. S. Nowick, Acta Met. **9**, 85 (1961).

[20] R. W. Dreyfus and A. S. Nowick, J. Appl. Phys. **33**, 473 (1962).

VI. DISCUSSION

The preceding analysis of the anelastic loss peaks provides values for the Na^+-vacancy jump rates w_1, w_3, and w_4, and an indication that w_2 is much smaller than these jump rates. Strong support for the small value of w_2 and, therefore, for the complete scheme of present identification of the normal modes, comes from data on Ca^{++} diffusion in NaCl. Specifically, the results of Banasevich, Lur'e, and Murin[21] show that diffusion of Ca^{++} ions in NaCl occurs with an activation energy of 0.9 eV. In view of the fact that *reorientation* of the impurity-vacancy complex by jumps of the Na^+ ion requires only 0.7 eV, as demonstrated by the relaxation measurements, it becomes clear that impurity-vacancy interchange, rate w_2, must limit the rate of diffusion. It is therefore clear that the comparatively high value for the activation energy for Ca^{++} diffusion supports the present conclusion, i.e., that w_2 is much smaller than the rates at which the vacancy jumps around the impurity. The diffusion data[22] for Mn^{++} do not establish that w_2 is negligible for this impurity; however, the extrapolation of these data into the low-temperature region does suggest that $w_2<w_1$.

It is interesting to consider the implications of the jump rates given in Table III, specifically, the fact that w_3 and w_4 are considerably larger than w_1. It should be recognized that a n.n. pair may reorient into another n.n. position in either of two ways: (a) A type-4 jump followed by a type-3 jump, or (b) a single type-1 jump. The present result then strongly favors the indirect path (a) as the most probable means of n.n. dipole reorientation. It is possible to understand why $w_4>w_1$ in terms of the displacements of the anions. The excess charge on a substitutional Ca^{++} or Mn^{++} ion attracts the six neighboring Cl^- ions radially inward. Since this displacement of the anions does not provide additional space for the type-1 jump, its influence is probably only of second order. On the other hand, as a result of the anion displacements, the Na^+ ion executing a type-4 jump (or its inverse type-3) moves through a dilated portion of lattice. It seems reasonable on this basis that w_4 turns out to be greater than w_1.

The ratio of w_3/w_4 provides an experimental value for the relative n.n. to n.n.n. populations and, therefore, binding energies.[5] Specifically,

$$\epsilon_{nn}-\epsilon_{nnn}=kT\ln(w_3/w_4), \tag{24}$$

where ϵ_{nn} and ϵ_{nnn} are the nearest- and next-nearest-neighbor binding energies, respectively. A comparison of the present results with theoretical and experimental results of other workers is given in Table IV.

TABLE IV. Values for $\epsilon_{nn}-\epsilon_{nnn}$ from various sources (in eV).

	NaCl:$CaCl_2$	NaCl:$MnCl_2$
Present results	0.044±0.006	0.020±0.011
From spin resonance[a]	···	0.034
From theory[b]	0.02	···

[a] Reference 18.
[b] Reference 17.

In the earlier work[3] the variation of the dielectric relaxation rate ${}_2\zeta_E$ with size of the divalent impurity in NaCl led to the conclusions summarized in the Introduction. The fact that the dielectric relaxation rate increased with decreasing size of the impurity ion was interpreted as due to the dominance of the type-1 jump for the larger ions, and the expectation that the type-2 jump would begin to enter appreciably as the ionic radius decreased. In the light of the more complete information now available, it is necessary to revise this conclusion. The present results show that the type-4 jump is the rate-determining step for the dielectric relaxation. The effect of impurity radius must therefore be interpreted as due to an increase in w_4 with decreasing impurity-ion radius. Finally, the earlier conclusion that the fraction of vacancies occupying n.n.n. sites increases as the radius of impurity ion decreases, is re-enforced by the present results. Specifically, the relative peak height for the relaxation identified by the rate ${}_1\zeta_{s'}$ increases appreciably in going from Ca^{++}- to Mn^{++}-doped samples. Since this peak is due primarily to n.n.n. pairs, it serves to illustrate the point in question. Additional support for this conclusion comes from the values of $\epsilon_{nn}-\epsilon_{nnn}$ given in Table IV.

ACKNOWLEDGMENTS

The authors wish to thank A. S. Nowick for extensive discussions and suggestions. Many helpful discussions with B. S. Berry and W. R. Heller are also acknowledged.

[21] S. N. Banasevich, B. G. Lur'e, and A. N. Murin, Fiz. Tverd. Tela **2**, 80 (1959) [English transl.: Soviet Phys.—Solid State **2**, 72 (1960)].
[22] B. G. Lur'e, A. N. Murin, and R. F. Brigevich, Fiz. Tverd. Tela **14**, 1957 (1962) [English transl.: Soviet Phys.—Solid State **4**, 1432 (1963)].